polymer papers

The structure of liquid crystalline copolyesters prepared from 4-hydroxybenzoic acid, 2,6-dihydroxy naphthalene, and terephthalic acid: 2. Atomic models for the copolymer chains*

Genaro A. Gutierrez, John Blackwell and Robin A. Chivers
Department of Macromolecular Science, Case Western Reserve University, Cleveland, Ohio 44106, USA
(Received 11 November 1983)

The X-ray fibre patterns from copolyesters of 4-hydroxybenzoic acid, 2,6-dihydroxynaphthalene, and terephthalic acid show meridional maxima that are aperiodic. The positions of these peaks can be reproduced by calculation of the scattering characteristics of copolymer chains of random sequence modelled as linear arrays of points, where each point represents a monomer separated from adjacent points by the appropriate monomer lengths. By introducing atomic models for the monomers, good agreement is also obtained between the observed and calculated intensities. It is shown that the intensity agreement is improved by refinement of the orientation of the monomers with respect to the fibre axis.

(Keywords: liquid crystalline polymers; X-ray diffraction; polymer structure; copolyesters; sequence distribution)

INTRODUCTION

In a previous paper[1] we made an initial investigation of the structure of the wholly aromatic copolyesters prepared from 4-hydroxybenzoic acid (HBA), 2,6-dihydroxynaphthalene (DHN), and terephthalic acid (TPA). These copolymers are thermotropic and can be melt-processed as high strength fibres or novel moulded plastics. X-ray fibre diagrams of the melt-spun fibres (*Figures 1* and *2*) show a high degree of axial orientation. Diffuse equatorial scatter shows that the lateral packing is largely disordered, but the presence of some three-dimensional order is indicated by some sharp Bragg maxima both on and off the equator. A most interesting feature of the diffraction data is that the meridional maxima are aperiodic and also shift in position with changes in the monomer ratio. We showed that the positions of these maxima can be reproduced by a model consisting of chains of completely random sequence, in which successive residues are represented by points separated by the appropriate residue lengths. Not only was good agreement obtained between the observed and calculated meridional d-spacings, but the calculations also reproduced a characteristic diffraction feature for these copolymers: a doublet at 3.5–3.0 Å that becomes more separated as the HBA content is decreased.

As will be described below, we have now extended these calculations to an atomic model for the copolymer chain in order to consider the match between the observed and calculated intensities. The meridional intensity depends on the projection of the structure onto the fibre axis. This projection is approximately independent of the chain conformation since the linkage bonds of the 1,4-phenylene and 2,6-naphthylene units are approximately parallel to the fibre axis. The methods used to calculate the meridional intensity distribution for an array of aperiodic polymer chains have been described in detail elsewhere[2]. For the point model our procedure was to set up a random copolymer chain of n monomers and calculate its Fourier transform, F_c, as follows:

$$F_c(Z) = \sum_{j=1}^{n} \exp(2\pi i Z z_j) \qquad (1)$$

where Z is the coordinate in reciprocal space in the direction corresponding to the chain axis, and z_j is the coordinate of the jth point monomer. The intensity was then calculated by averaging over N chains:

$$I(Z) = \sum_{c=1}^{N} |F_c(Z)|^2 \qquad (2)$$

In ref. 1, $I(Z)$ was averaged over 250 chains of 40 residues. The length of the chain corresponds more to a persistence length of the stiff chain rather than a true degree of polymerization, which is reported[3] to be approximately 150. This approach was also used effectively for copolymers of HBA and 2-hydroxy-6-naphthoic acid, in which the transforms were calculated by averaging over 200 chains of 15 monomers[4]. Recent calculations for the latter system have shown that the line profile at $d \simeq 2.1$ Å is sensitive to the persistence length, and that the best agreement is obtained for chains of 9–13 residues, depending on the monomer composition[5].

Use of a random number generator leads to statistical variations in the results due to the limited sample size. These could be eliminated by considering all possible

* Paper 1 of this series is reference 1

0032-3861/85/030348-07$03.00

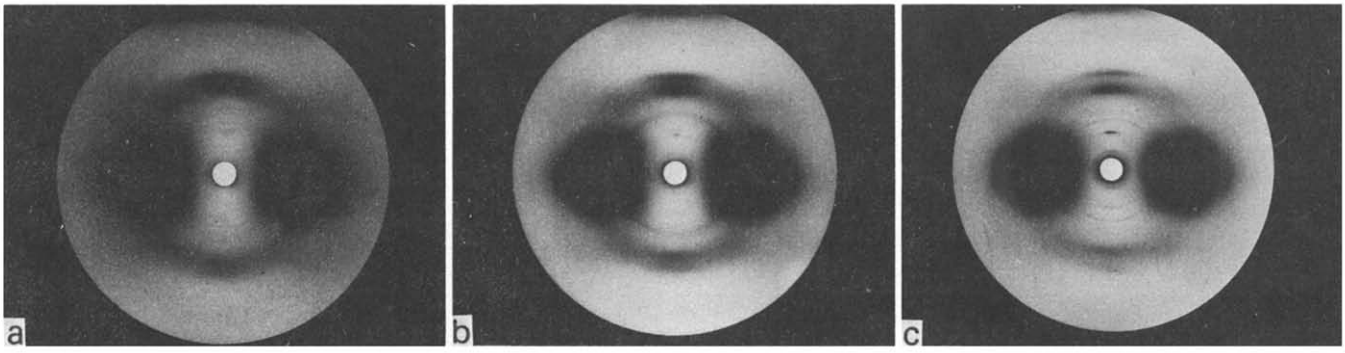

Figure 1 X-ray diffraction fibre diagrams of HBA/DHN/TPA copolyesters of three different molar compositions: (a) 60/20/20, (b) 50/25/25, and (c) 40/30/30. The fibres are tilted slightly with respect to the chain axis from the position perpendicular to the X-ray beam

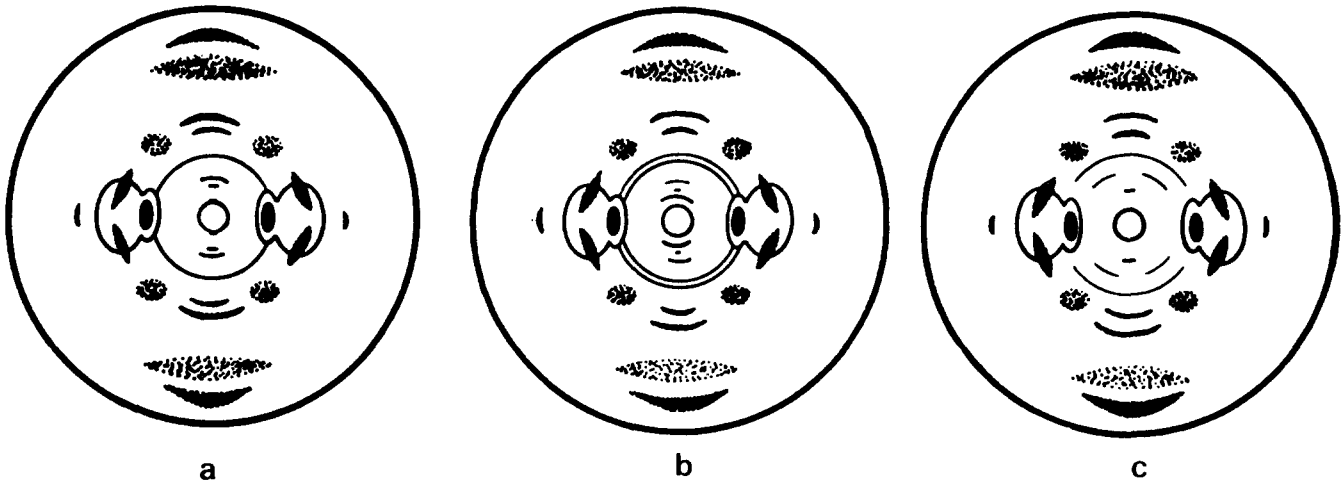

Figure 2 Schematics of the X-ray fibre diagrams of the HBA/DHN/TPA copolymers shown in *Figure 1*. The molar compositions are: (a) 60/20/20, (b) 50/25/25, and (c) 40/30/30

copolymer sequences:

$$I(Z)=\sum_{c=1}^{N} P_c|F_c(Z)|^2 \tag{3}$$

where P_c is the probability of that particular sequence. This calculation is simplified by making use of the autocorrelation function, $Q(z)$, which is the probability of a neighbour at a separation of z along the chain. $I(Z)$ is then given by:

$$I(Z)=\sum_j Q(z_j)\cos(2\pi Z z_j) \tag{4}$$

where the summation is over all neighbour separations. Note that $Q(z)$ is centrosymmetric because there are equal probabilities of neighbours in both directions along the chain.

For an atomic model, equation (4) becomes:

$$I(Z)=\sum_j\sum_k Q(z_{jk})f_j f_k \exp(2\pi i Z z_{jk}) \tag{5}$$

where $Q(z_{jk})$ is the probability of an atom pair, j and k, separated by z_{jk}. Equation (5) is simplified by separation of the point autocorrelation function $Q(z_l)$ into its components:

$$Q(z_l)=\sum_A\sum_B Q_{AB}(z_l) \tag{6}$$

where $Q_{AB}(z_l)$ is the probability of residue A and residue B at a separation z_l, i.e. residue A at the origin and residue B at z_l. Equation (5) now becomes:

$$I(Z)=\sum_A\sum_B Q_{AB}(z_l)F_{AB}(Z)\exp(2\pi i Z z_l) \tag{7}$$

$F_{AB}(Z)$ is the Fourier transform of the convolution of residue B with residue A:

$$F_{AB}(Z)=\sum_j\sum_k f_{A,j}f_{B,k}\exp[2\pi i Z(z_{A,j}-z_{B,k})] \tag{8}$$

where the subscripts, A,j and B,k, designate the jth atom in residue A and the kth atom in residue B, respectively, when both residues are located at the origin.

For the terpolymer studied here, there are sixteen $F_{AB}(Z)$ species, corresponding to all the pair combinations of HBA, DHN and TPA. (Note that there is a sense to the HBA residue with a result that the 'up' and 'down' residues need to be treated as separate entities.) The self-convolutions, $F_{AA}(Z)$, are real; the other $F_{AB}(Z)$ terms, i.e. the cross-convolutions, are complex, but the imaginary components in equation (7) are eliminated as a consequence of $F_{AB}(Z)=F^*_{BA}(Z)$ (i.e. they are complex conjugates) and $Q_{AB}(z)=Q_{BA}(-z)$. Results for both the point and atomic models of the HBA/DHN/TPA copolymers are presented below.

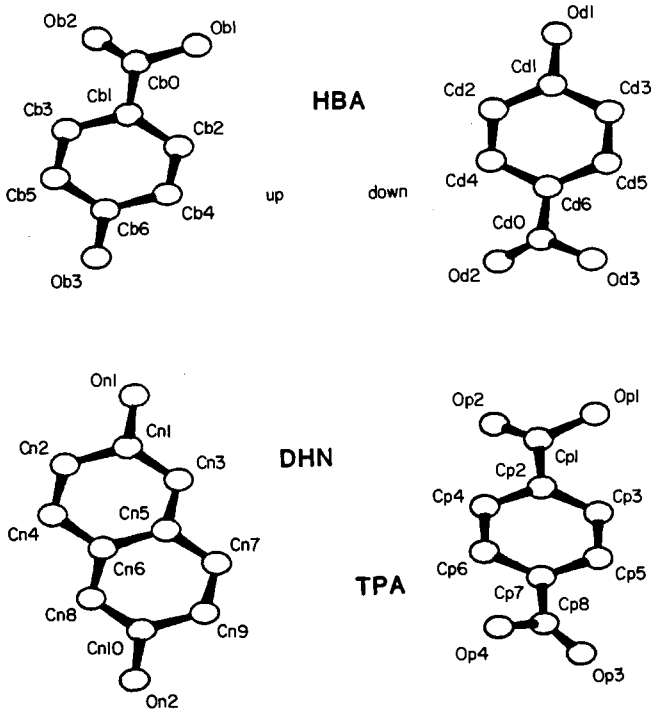

Figure 3 Projections of the molecular models for the HBA, DHN and TPA residues. The plane of the carboxyl group is rotated 30 degrees with respect to the benzene ring in HBA (up and down) and TPA

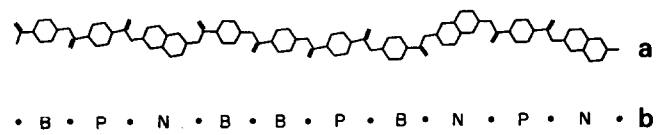

Figure 4 (a) A short sequence of random chain molecule of HBA/DHN/TPA, and (b) its equivalent point model

EXPERIMENTAL

Melt-spun fibres of the HBA/DHN/TPA copolymers were obtained from Celanese Research Company, Summit, NJ, in the following monomer ratios, 60/20/20, 50/25/25 and 40/30/30, and had been synthesized as described by Calundann[3]. X-ray fibre diagrams were recorded on Kodak no-screen film using a Searle toroidal focusing camera and Ni-filtered CuKα radiation. The d-spacings were calibrated with calcium fluoride. These X-ray patterns were published previously in ref. 1 and are shown in *Figure 1*. In view of the difficulties in reproduction, schematics of these patterns are shown in *Figure 2*. To facilitate comparison of the meridional intensities in the 3 Å region, X-ray patterns were recorded with the fibres inclined at 76° to the beam ($d \simeq 3.2$ Å intersecting the sphere of reflection) and linear densitometer scans of this region were obtained using a Joyce Loebl scanning microdensitometer.

Models for the monomer residues were set up using standard bond lengths and angles, in keeping with the known structures of low molecular weight aromatic esters[6,7]. The individual phenylene, naphthylene and carboxyl groups were assumed to be planar, and hence the chain conformation is determined by the aromatic-carboxyl torsion angles, χ. In our models (shown in *Figures 3* and *4*), the inclination of the aromatic and carboxyl groups was set at 30°, as suggested by structural work on comparable polyesters and polyamides[8,9]. This inclination is achieved by four possible values of $\chi = \pm 30$ and ± 150. For a starting model the residues were arranged with the ester oxygen–ester oxygen vectors parallel to the chain axis. The residue lengths, l_r, of the HBA and DHN are 6.35 and 7.85 Å, respectively, and their axial projections are independent of χ. For TPA there are four possible axial lengths: 6.75, 6.87, 7.15 and 7.26 Å, for the different possible combinations of the two χ angles. In principle we need to consider a distribution of these four possibilities. For the present purposes we have used the 7.15 Å model to represent the average TPA residue. The atomic coordinates for the residues are given in *Table 1*, and projections of their structures are shown in

Table 1

Atomic coordinates	x	y	z
*HBA (up)**			
Ob1	0.0000	0.0000	0.0000
Ob2	0.0162	−2.2369	0.2985
Cb0	0.0000	−1.1379	0.7648
Cb1	−0.0226	−0.8033	2.2135
Cb2	−0.6271	0.3537	2.7196
Cb3	0.5977	−1.7072	3.0844
Cb4	−0.6112	−0.6067	−4.0964
Cb5	−0.6134	−1.4542	−4.4612
Cb6	0.0090	−0.2972	4.9673
Ob3	0.0000	0.0000	6.3486
*HBA (down)**			
Od1	0.0000	0.0000	0.0000
Cd1	0.0000	−0.2973	1.3814
Cd2	0.5692	−1.4720	−1.8874
Cd3	−0.5926	0.6249	2.2522
Cd4	0.5458	−1.7244	3.2643
Cd5	−0.6160	0.3724	3.6290
Cd6	−0.0468	−0.8022	4.1351
CdO	−0.0344	−1.1373	5.5838
Od2	−0.0513	−2.2364	6.0501
Od3	0.0000	0.0000	6.3486
DHN			
On1	0.0000	0.0000	0.0000
Cn1	0.0000	−0.1405	1.4060
Cn2	0.0000	−1.4619	1.8686
Cn3	0.0000	0.9208	2.3191
Cn4	0.0000	−1.7220	3.2442
Cn5	0.0000	0.6607	3.6946
Cn6	0.0000	−0.6607	4.1572
Cn7	0.0000	1.7219	4.6077
Cn8	0.0000	−0.9208	5.5329
Cn9	0.0000	1.4618	5.9834
Cn10	0.0000	0.1404	6.4459
On2	0.0000	0.0000	7.8519
TPA			
Op1	0.0000	0.0000	0.0000
Op2	0.2076	−2.2032	0.4426
Cp1	0.0000	−1.0925	0.8283
Cp2	−0.2883	−0.6941	2.2317
Cp3	−1.0858	0.4078	2.5631
Cp4	0.2786	−1.4776	3.2440
Cp5	−1.3162	0.7263	3.9067
Cp6	0.0480	−1.1592	4.5877
Cp7	−0.7493	−0.0572	4.9191
Cp8	−1.0376	0.3412	6.3225
Op3	−2.0279	0.8857	6.7081
Op4	0.0000	0.0000	7.1504

* In contrast with the DHN and TPA residues, HBA possesses directionality due to its chemical asymmetry, i.e., it can react through its carboxyl or hydroxyl end, thus generating two different sets of atomic coordinates

Figure 3 with 'up' and 'down' HBA residue being treated as separate entities. In later calculations for the atomic model the effect of nonlinearity of the residues (i.e. where the ester oxygen–ester oxygen vector was inclined rather than parallel to the chain axis) was considered by tilting the residues at a specified angle, with a consequent reduction in the length of the axial projection.

The theoretical intensities are calculated for a normal distribution of chain lengths with average length 12 monomers ($\sigma = 1.33$) which corresponds to an average persistence length of approximately 85 Å. The data for the atomic model were corrected for Lorentz and polarization effects, assuming the geometry of a $\theta/2\theta$ diffractometer scan.

RESULTS AND DISCUSSION

The calculated meridional intensity distribution for the three monomer ratios are shown in *Figures 5a, b* and *c*. In each case we present the data for the point and atomic models in which the residues (i.e. the ester oxygen–ester oxygen vectors) are parallel to the chain axis, and for an atomic model in which the residues have been tilted with respect to the chain axis (as detailed below) in order to improve the match between the observed and calculated intensities. The d-spacings for the observed and calculated maxima are given in *Table 2*.

The calculated intensity distributions for the point model, derived as the Fourier transform of the autocorrelation function, $Q(z)$, for totally random sequences, contain peaks at positions that are in good agreement with the observed maxima. These data are comparable to those obtained using the random number approach[1], but are not subject to the statistical variations due to the limited sample size. (Some of the minor differences between these results and those reported previously are also due to the use of slightly different monomer lengths.) The observed positions of the strong maximum at $d \simeq 2.0$ Å and the strong doublet in the 3.0–3.5 Å region are reproduced to within 0.1 Å. An intense maximum is predicted at $d \simeq 7$ Å, which encompasses the one or two

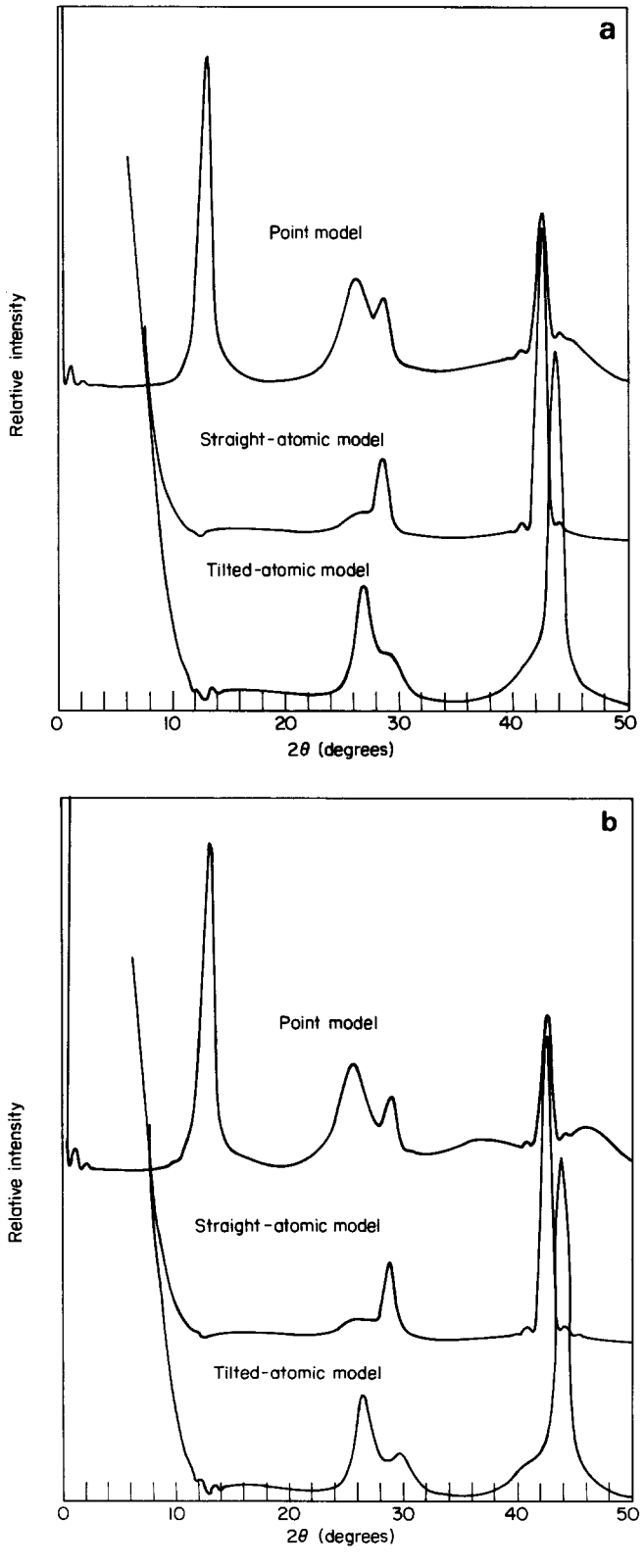

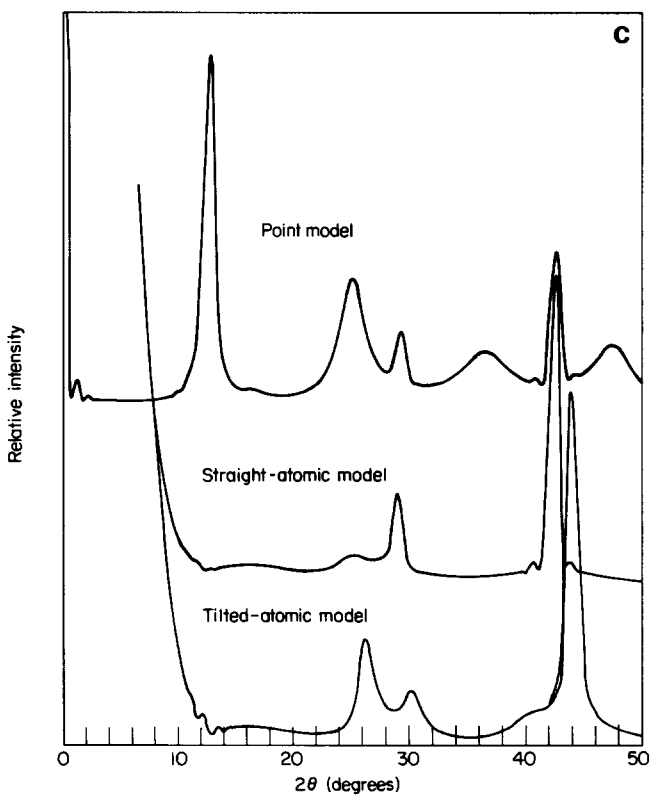

Figure 5 Calculated meridional intensity distributions for HBA/DHN/TPA copolymers of three different compositions: (a) 60/20/20, (b) 50/25/25, and (c) 40/30/30. In each case the results are shown for the point, straight-atomic and tilted-atomic models (see text). The calculations are based on chains of random sequence containing an average of 12 residues ($\sigma = 1.33$)

Table 2

Composition (mol %)	*d*-spacings (Å)			
		Calculated		
HBA/HNA/TPA	Observed*	Point model	Straight-atomic model	Tilted-atomic model
60/20/20	6.8 w	6.81	7.25	7.05
	6.05 w		6.45	6.37
	3.31 s	3.38	3.28	3.29
	2.98 s	3.11	3.11	3.06
	2.3 w, b			
	2.01 s	2.13	2.13	2.07
50/25/25	6.98 w	6.95	7.35	7.10
	5.9 w		6.63	6.41
	3.38 s	3.47	3.40	3.34
	2.97 s	3.08	3.09	3.00
	2.3 w, b	2.42		
	2.02 s	2.13	2.13	2.06
40/30/30	6.96 w	7.05	7.47	7.15
				6.46
	3.48 s	3.56	3.50	3.38
	3.06 s	3.06	3.07	2.94
	2.3 w, b	2.46		
	2.0 s	2.13	2.13	2.05

* Relative intensities are denoted as: w = weak; b = broad; s = strong

weak maxima observed in this region. In addition, the theroetical curves for the point models show a broad maximum at $d \simeq 2.3$ Å, and weak diffuse intensity is seen in this region on the fibre diagrams, although, as will be discussed below, it is not clear whether this is on or off the meridian.

In the first calculations for an atomic model, we used models for the residues with the ester oxygen–ester oxygen vectors parallel to the chain axis. The calculated transforms show maxima in approximately the same positions as those for the point models. For each copolymer composition, the most intense maximum is at $d \simeq 2.1$ Å, followed by the doublet in the range $d \simeq 3.0$–3.5 Å. The strong maximum at $d \simeq 7$ Å for the point model has been replaced by a very weak doublet as is observed for the 60/20/20 and 50/25/25 compositions. (*NB* all the subsidiary maxima in this region have been eliminated by averaging over a distribution of chain lengths.) The breadth of the central peak is an artifact due to the use of a short chain to model the short persistence length in much longer molecules. The broad peak at $d \simeq 2.3$ Å predicted for the point model is not predicted for the atomic model, and it may be that the intensity in this region is off the meridian but is arced onto the meridian due to fibre disorientation. This will be addressed further in future work when the three-dimensional structure is considered.

Thus the major effect of conversion from the point to the atomic model is to improve the agreement between the observed and calculated intensities. There have been no major shifts in the positions of the maxima and no unacceptable elimination of old peaks or generation of new ones. These data confirm our original view that the diffraction pattern is approximately the transform of the aperiodic point lattice but with the intensities modulated by the transform of an 'average' monomer, and demonstrate the utility of the point residue approximation for investigating the structure of stiff chain polymers.

The effect of intraresidue interferences increases the

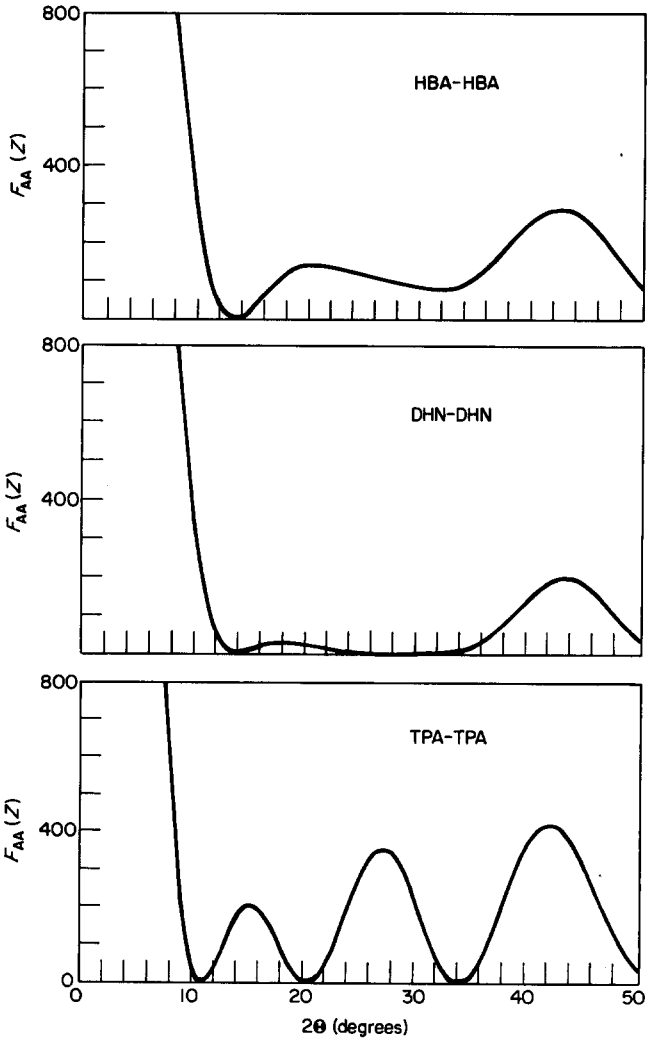

Figure 6 Fourier transforms of the monomer self-convolutions, $F_{AA}(Z)$

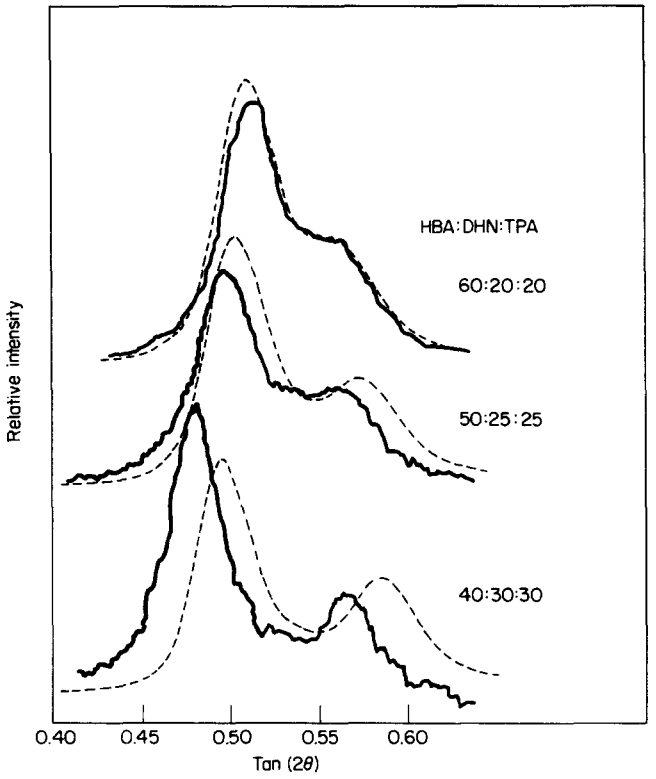

Figure 7 Meridional intensity distribution in the 3.5–3.0 Å region for HBA/DHN/TPA copolymers of three different compositions: 60/20/20, 50/25/25 and 40/30/30. Optical densitomer scans are drawn as solid lines. The dashed lines show the intensity calculated using the tilted-atomic model. Tilt angles are 5, 25 and 10 degrees for HBA, DHN and TPA respectively

intensity at $d \simeq 2.1$ Å, and greatly reduces the intensity at $d \simeq 7$ Å, where one maximum is converted into a doublet. The origin of these effects is seen in *Figure 6*, which shows the Fourier transforms of the monomer self-convolutions, $F_{AA}(Z)$. These have minima at $d \simeq l_r$ (the residue length), i.e. $d \simeq 6$ to 8 Å, and then fluctuate up to a maximum at $d \simeq 2$ Å. The intensity for the atomic model is the weighted product of these terms (and the cross terms, $F_{AB}(Z)$) with the Fourier transform of the point correlation function in equation (7).

Nevertheless, closer comparison of the observed and calculated intensity distribution shows that there is poor agreement for the 3 Å doublet. Specifically, the inner maximum is predicted to be weaker than the outer maximum, whereas the reverse is observed for all three compositions. *Figure 7* shows optical densitometer scans of the 3 Å meridional region of the diffraction pattern for all three compositions. These data were recorded for fibres tilted for a meridional at $d \simeq 3.2$ Å (i.e. with the fibre axis at 76° to the beam) and hence distortion due to curvature of the sphere of reflection should be minimal.

The deficiency in the model responsible for these intensity differences could arise from our assumption that all the residues are parallel to the chain axis. In fact, the ester oxygen–ester oxygen vectors must be distributed about the chain axis, as can be seen in the typical random sequence in *Figure 3*. The latter diagram was generated setting all the aromatic–carboxyl interplanar angles at $\chi = \pm 30°$. In the actual structure a distribution of torsion angles is to be expected, which will lead to an even larger distribution of tilt angles for the residues.

We have modelled this effect by inclining the individual residues at different angles to the chain axis. Naturally, if all three types of residue are tilted at the same angle, then the only effect is a proportional shift in the positions of the maxima, and the relative intensities are unchanged. However, from study of models of random chains such as that shown in *Figure 3*, it appears likely that the DHN residues will be tilted more than the others, because of the off-set 2,6 linkage bonds. The HBA residue is least likely to be tilted, with TPA intermediate between the two. We have considered the effects of residue tilting by fixing the residues at a number of different tilt angles. The results presented here are for HBA tilted by 5°, TPA by 10°, and DHN by 0° to 30° in 5 increments. *Figures 8* and *9* show the calculated meridional intensities for point and atomic models for the 60/20/20 monomer ratio as a function of DHN tilt angle, respectively.

Tilting the residues has relatively little effect on the $F_{AB}(Z)$ terms (e.g. those in *Figure 6*). The major effects are seen in the point model interference functions, and these arise as a result of the relative changes in the monomer lengths. It can be seen in *Figure 8* that as the DHN tilt angle increases there is an increase in the intensity of the inner peak of the doublet, and a decrease in that of the outer peak, which has become very weak at a tilt of 20°. This behaviour is reflected in the transforms of the atomic model (see *Figure 9*), where progressive tilting of the DHN

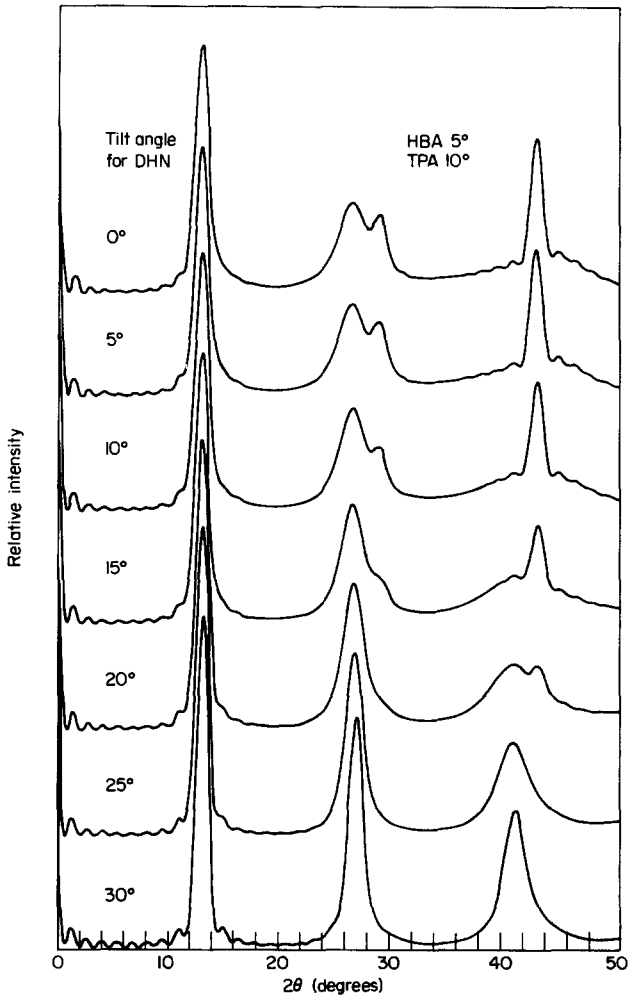

Figure 8 Calculated meridional intensity distributions for point models of the 60/20/20 HBA/DHN/TPA copolymer at different DHN tilt angles. Tilt angles for the HBA and TPA residues were set at 5 and 10 degrees, respectively

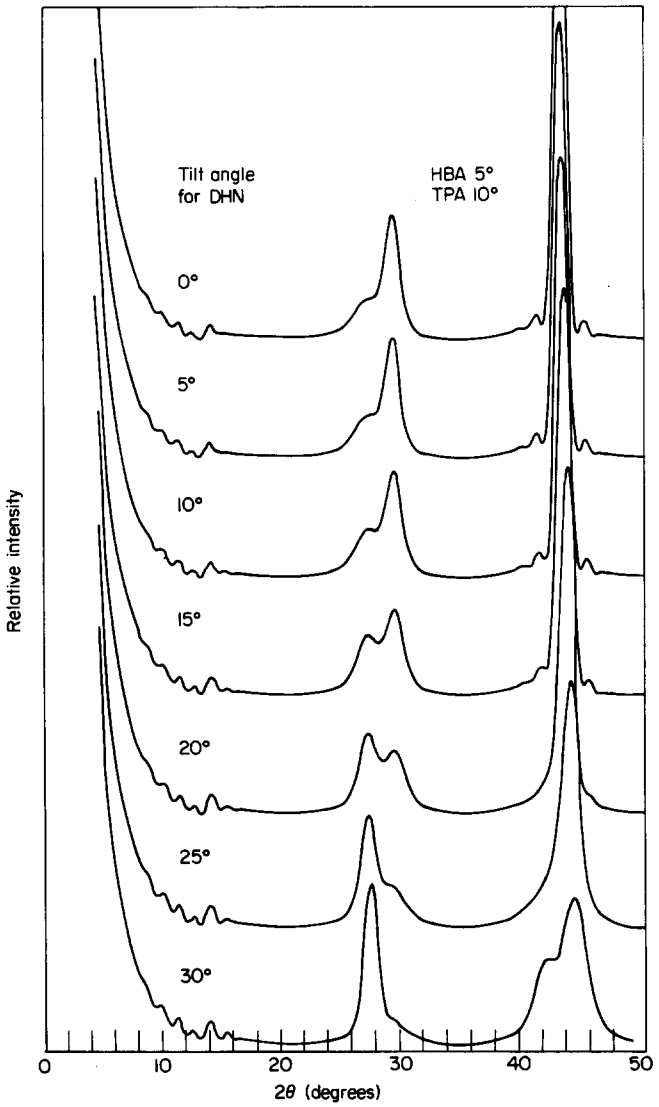

Figure 9 Calculated meridional intensity distributions for atomic models of the 60/20/20 HBA/DHN/TPA copolymer at different DHN tilt angles. Tilt angles for the HBA/DHN/TPA residues were set at 5 and 10 degrees, respectively

residue results in a reversal in the relative intensity of the inner and outer maxima. The best agreement is obtained for a tilt of 25° in DHN, and this is found to be the case also for the other two compositions. The transforms for the 25° tilted-atomic model for all three compositions are shown in *Figure 5*. These data in the 3 Å region are also shown in *Figure 7*, where they can be seen to be in very good agreement with the observed densitometer scans. Some of the $F_{AB}(Z)$ terms in equation (5), notably the TPA self-convolution and the TPA–HBA cross-convolution functions, increase sharply between $d = 3.5$ and 3.0 Å, and this accounts for the reversal of intensity of the doublet on conversion from the point to the atomic model. It is interesting that the calculations also reproduce the greater angular breadth of the inner component of the doublet.

Tilting the residues leads to a more reasonable model for the chain that gives better agreement with the observed intensities. However, these results only illustrate one method of refining the model. A more rigorous approach would be to incorporate a distribution of both residue tilts and torsion angles followed by a point by point comparison of the observed and calculated intensities. Such calculations are feasible, but the problem is complicated by the presence of some three-dimensional order, i.e. a preference for a specific axial stagger of adjacent chains in a fraction of the specimen. This will lead to additional interference effects that may modulate the meridional intensities from those calculated with the present model. (The above treatment assumes random axial stagger, as is likely in the regions without three dimensional order.) The results described here are presented to show that refinement of the monomer orientation can lead to improvement in the intensity agreement. To proceed further we need to derive a three-dimensional model in order to incorporate the effects of interchain interferences, and this will be the subject of a future paper.

ACKNOWLEDGEMENTS

This research is supported by N.S.F. grants DMR81-19425 (Materials Research Laboratory) and DMR81-07130 (from the Polymer Program). We thank Celanese Research Company for supplying the specimens of the liquid crystalline copolyester fibres and for very useful discussions.

REFERENCES

1 Blackwell, J. and Gutierrez, G. A. *Polymer* 1982, **23**, 671
2 Blackwell, J., Gutierrez, G. A. and Chivers, R. A. *Macromolecules* 1984, **17**, 1219
3 Calundann, G. W. (Celanese), US Pat. 4 184 996 (1980)
4 Gutierrez, G. A., Chivers, R. A., Blackwell, J., Stamatoff, J. B. and Yoon, H. *Polymer* 1983, **24**, 937
5 Chivers, R. A., Blackwell, J. and Gutierrez, G. A. *Polymer* 1984, **25**, 435
6 Adams, B. J. and Morsi, S. E. *Acta Crystallogr.* 1976, **B32**, 1345
7 Pattabhi, V., Raghunathan, S. and Chacko, K. K. *Acta Crystallogr.* 1978, **B34**, 3118
8 Northolt, M. G. and van Aartsen, J. J. *J. Polym. Sci., Polym. Lett. Edn.* 1973, **11**, 333
9 Tashiro, K., Kobayashi, M. and Tadokoro, H. *Macromolecules* 1977, **10**, 413